Gondwana Research 108 (2022) 22–30

Contents lists available at ScienceDirect

Gondwana Research

journal homepage: www.elsevier.com/locate/gr

Characterization of microplastics in sediment using stereomicroscopy and laser direct infrared (LDIR) spectroscopy

Yi-Ling Cheng [a,1], Ruijie Zhang [a,b,1], Louis Tisinger [c], Salvatore Cali [a], Zhou Yu [d], Hua Yun Chen [a], An Li [a,*]

[a] School of Public Health, University of Illinois at Chicago, Chicago, IL, United States
[b] Guangxi Laboratory on the Study of Coral Reefs in the South China Sea, Coral Reef Research Center of China, School of Marine Sciences, Guangxi University, Nanning 530004, China
[c] Life Science and Chemical Analysis, Agilent Technologies, Inc., Wood Dale, IL, United States
[d] Department of Mathematics, Statistics, and Computer Science, University of Illinois at Chicago, Chicago, IL, United States

ARTICLE INFO

Article history:
Received 24 May 2021
Revised 3 October 2021
Accepted 5 October 2021
Available online 9 October 2021

Keywords:
Microplastics
Sediment
Laser direct infrared (LDIR) spectroscopy
Lake Michigan

ABSTRACT

The analysis of microplastics (MP) becomes more difficult for smaller sizes, especially in complex matrices such as sediment of natural waters. In this work, we analyzed MPs in sediment using laser direct infrared (LDIR) imaging, a relatively new technique in environmental MP studies. Sediment samples were spiked with analytical surrogates (polyethylene spheres), and subjected to density separation, wet peroxide oxidation, calcite removal, and filtration. The extracted particles were coated on to a low-emissivity glass slide which was first examined on a stereomicroscope. Six slides (two sediment samples and four different blanks) were further analyzed using an Agilent LDIR system. Approximately 520 and 430 MP/g were found in the two samples, with diameter ranging 20–3384 μm and 84% being smaller than 100 μm. The increase in particle count with decreasing particle sizes followed a power law curve, suggesting that a large portion of the smaller MPs was generated by the breakdown of larger plastic pieces. Major polymers found in this work included polyamide, polyester, polytetrafluoroethylene, and polyacetal. Most MPs were fragments, while beads and fiber were also found. In the two sediment samples, 14% and 46% of the total particles, respectively, were composed of non-plastic micro-sized particles, including natural polyamide, cellulose, chitin, rubber, and "unknown". Challenges, potential biases, and uncertainties are discussed. This work is the first application of LDIR imaging on MPs in natural sediment.

1. Introduction

Plastic debris, large or small, occurs throughout the water column in rivers, lakes and oceans. Many plastics have densities greater than that of water thus the particles may sink naturally. Biomass accumulation (biofouling) and adsorption of minerals and other materials may also contribute to increased density and loss in buoyancy (Andrady, 2011; Kaiser et al., 2017; Moret-Ferguson et al., 2010; Reisser et al., 2013; Zettler et al., 2013). It has been estimated that 70% of plastic debris entering the oceans ultimately sink (Driedger et al., 2015). Modeling results for ocean water suggest that particles with diameter 100 μm need only 10 (polyvinyl chloride) to 160 (polystyrene) days to sink 4000 m (Kooi et al., 2017). Therefore, it is reasonable to hypothesize that sediments have accumulated a large proportion of plastics in natural waters, especially in lakes with long water residence times.

Reliable characterization and quantitative assessment of MPs in sediment of natural waters are challenging, and the difficulties increase as MP size decreases (Isobe et al., 2019; Law and Thompson, 2014; Van Cauwenberghe et al., 2015). MPs are most commonly defined as plastic particles with diameter between 1 μm and 5 mm, although an upper limit of 1 mm for the longest dimension has been suggested (Browne et al., 2011; Kane et al., 2020). The ranges of particle sizes and densities may overlap between MPs and many non-plastic particles in sediment, including naturally occurring polymers and pollutant particles, making separation and cleanup processes challenging. Additionally, settling particles in natural waters are often heteroaggregates with inorganic (e.g., fly ash and black carbon) and organic (e.g., natural organic matter) constituents that, if not properly removed, could obstruct the identification of the synthetic polymers and affect the particle counting (Alimi et al., 2018).

Laser Direct Infrared (LDIR) is a new technique for chemical imaging, infrared (IR) microscopy, and IR spectral analysis. Currently widely used Fourier transform infrared (FTIR) microscopes use focal plane array (FPA) imaging technology to spread light over an area and look at multiple particles simultaneously, and needs

* Corresponding author.
E-mail address: anli@uic.edu (A. Li).
[1] Yi-ling Cheng and Ruijie Zhang are co-first authors. They contributed equally.

https://doi.org/10.1016/j.gr.2021.10.002
1342-937X/

>30 sec to produce a typical IR spectrum (Kole and Mainali, 2019). In comparison, the LDIR utilizes tunable quantum cascade laser (QCL) as the IR source, targets and focuses on particles, and ignores empty spaces. It is able to produce stronger signals with faster speed than the FTIR FPA imaging systems, and it does not use liquid nitrogen. LDIR is being adopted for environmental research; however, a literature search has found only two journal research articles using this technique for environmental MPs (Li et al., 2021; Scircle et al., 2020).

The objective of this study was to investigate the feasibility of using LDIR to characterize the MP particles in natural sediment. A total of eight surface grab sediment samples from Lake Michigan were processed. Particle as small as 20 μm (μm) in diameter in two of the samples and various blanks were characterized and quantified by LDIR. All samples were examined for the recoveries of added surrogate MP particles using a stereomicroscope. Potential interferences by non-plastic particles from the sediment were examined.

2. Materials and methods

2.1. Chemicals and materials

Zinc chloride (purity ≥ 97%), iron (II) sulfate heptahydrate (ACS grade, purity 99+%), 30% hydrogen peroxide (purity 30.0–32.0%), 37.2% hydrochloric acid (purity 36.5–38.0% w/w), and methanol (purity ≥ 99.9%) were purchased from Fisher Scientific (Bridgewater, NJ).

Two types of colored polyethylene (PE) microspheres, including red (0.98 g/cc, 180–212 μm) and green (0.98 g/cc, 106–125 μm), were purchased from Cospheric LLC (Santa Barbara, CA). They were chosen mainly based on expected size ranges involved in this work, intermediate density among various polymers, and their bright colors which would make their detection easy. A roll of 25 μm 316L stainless steel woven wire screen (500 mesh) was purchased from Beyondsupply Inc. through Amazon.com. It was cut into square (5.5 cm × 5.5 cm) pieces. MirrIR low emissivity (low-e) glass slides (25 mm × 75 mm) made by Kevley Technologies were purchased from Fisher Scientific. The MirrIR slides have no interfering absorptions in wavenumber range from 4000 to 400 cm^{-1} (Kevley Technologies).

2.2. Sediment samples

The sediment samples used in this work were collected from Lake Michigan in 2010, using a Ponar surface grab sampler on board of the US EPA Research Vessel (R/V) *Lake Guardian*. Each of the sediment samples was homogenized using a metal paint mixer, subsampled into a glass jar, and frozen immediately. Additional details of the sampling procedures can be found elsewhere (Li et al., 2018). The samples were previously freeze dried and analyzed for various organic pollutants (Cao et al., 2017; Guo et al., 2016; Guo et al., 2017; Guo et al., 2020; Li et al., 2018; Codling et al., 2014, 2018). The remaining dried samples had been stored in glass vials, which had thread caps with aluminum foil liners, in a laboratory refrigerator prior to this work.

For this work, eight of the 30 Ponar grab samples were selected based on sampling locations and sample availability (Table S1). Fig. 1 shows the locations of the eight sampling sites. All of these locations are in depositional zones, and included both northern and southern basins as well as the Green Bay of Lake Michigan.

2.3. Extraction and cleanup

We modified the laboratory procedure developed by NOAA (Masura et al., 2015) with references to the methods of Zobkov and Esiukova (Zobkov and Esiukova, 2017a; Zobkov and Esiukova, 2017b) and others (see the review by Van Cauwenberghe et al., 2015). The method development stage used archived sediment samples collected from other lakes. Our finalized procedure is illustrated in Fig. 2 and described below.

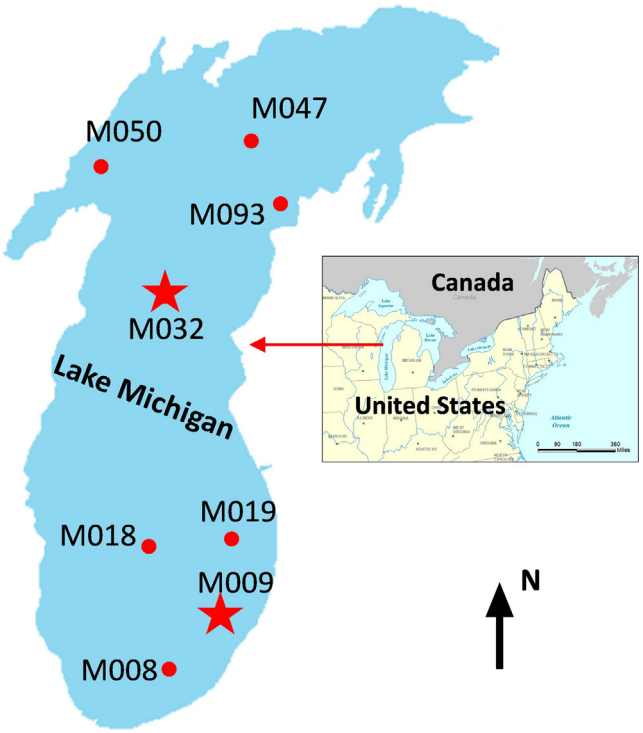

Fig. 1. Sample collection locations in Lake Michigan. Surface grab sediment samples from all the marked sites were examined using the AmScope stereomicroscope, and the two marked with stars were further characterized using the Agilent 8700 LDIR imaging system.

The dry mass of the samples extracted ranged from 20 to 30 g (Table 1). Each sample was weighed with an accuracy of 0.01 g in a glass beaker, and the red (n = 30) and green Cospheric PE spheres were added as recovery surrogate and size reference, respectively. Density separation was performed three times by adding to the beaker 100 mL, 50 mL, and 50 mL, respectively, of the $ZnCl_2$ solution (density = 1.6 g/mL). In each density separation step, the mixture was left undisturbed for at least 5 h for the layers to separate; then, the supernatant which contained MP particles was poured through a stainless-steel screen with 25 μm openings under vacuum to capture all the particles with diameters greater than 25 μm. The screen was clamped onto a no-frit support base of a MilliporeSigma™ 47 mm glass vacuum filtration bottle holder set. A rubber policeman was used to assist the transfer of particles. The beaker and the policeman were rinsed with the $ZnCl_2$ solution over the screen.

After the density separation, the MP particles retained on the screen was washed with a total of 60 mL hydrogen peroxide (H_2O_2) to a 600 mL beaker with 30 mL 0.05 M Fe (II) solution added in advance. After the bubbles in the solution diminished, the beaker was heated on a hot plate for 30 min at 75 °C. These steps were to remove organic particles and biofilms that might be present on the particles due to biofouling. Then, 30 mL 4.5% HCl was added to digest inorganic carbonates in mussel shells and sediment, which may not be removed entirely during extraction by $ZnCl_2$ and H_2O_2 treatment (Masura et al., 2015). The liquid mixture was then poured through the stainless-steel screen with vacuum. After being soaked in the beaker for a few minutes, the particles on the screen were washed by about 60 mL $ZnCl_2$ solution into a glass funnel, which was fitted with a latex tubing on the bottom of the stem and a pinch clamp, similar to the "density separator" used by

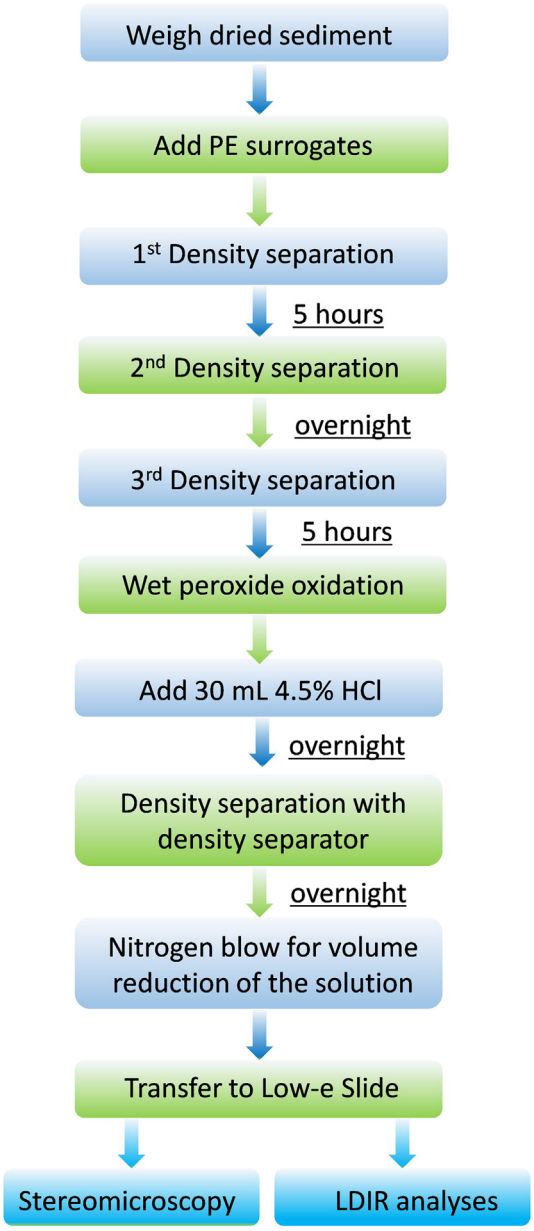

Fig. 2. Flow chart of sediment sample treatment Procedure.

Masura et al. (2015). After standing unagitated overnight, the settled denser layer of the mixture was drained and discarded. The remaining upper layer was poured through the same stainless-steel screen under gentle vacuum with the rinse of distilled water.

The microplastic particles on the screen were transferred to a 50 mL glass tube with screw cap, with the use of methanol. The volume of methanol was reduced by nitrogen blow while the glass tube was placed in a water bath at 68 °C on an N-EVAP nitrogen evaporation system (Organomation Associate Inc.). After carefully washing the wall of the glass tube, the particles along with a small volume of methanol were transferred slowly onto a MirrIR low-e glass slide. The methanol evaporated, leaving the particles deposited on the slide. The slides prepared using the steps described above were intended for both stereomicroscopic and LDIR analyses.

2.4. Stereomicroscope examination

Examination using a stereomicroscope has been recommended as a reasonable step prior to any analysis of MPs (Dris et al., 2018). In this work, a stereomicroscope (AmScope 7X-45X Dual Lit 6 W LED Trinocular Stereo Zoom Microscope) with a digital camera (AmScope MU500) was used to examine the finished MirrIR slides. The examination was facilitated by a grid with 15 × 5 cells printed in red ink on a transparency sheet, with each cell measured 7.5 m m × 7.5 mm. The sheet was placed under the MirrIR slide on the stereomicroscope when photos were taken. Each MirrIR slide covers about 40 cells. A colored photograph was taken for each cell. Close-up photos were taken at selected spots (Fig. 3).

2.5. Laser direct infrared (LDIR) imaging

The MirrIR slides were scanned on the Agilent 8700 LDIR imaging system at an Agilent facility near Chicago. Due to Covid-19 pandemic, the facility was closed after we finished six runs including four different blanks (see Section 2.7) and two sediment extract samples (M009 and M032). The operation of the instrument was automated with Agilent Clarity software version 1.1.23. This system is capable of measuring particles as small as 10 μm in diameter. Particles were counted and data for length, width, height, diameter, aspect ratio, area, perimeter, eccentricity, circularity, and solidity were compiled. The built-in spectral library for plastics was structured around an FTIR reference database design for the automated analysis of microplastic samples (Primpke et al., 2018). The quality of spectra matching was provided for each detected particle. The lowest percent match for the reported MP chemical identities was 65% as shown in Table S1 of the Supplementary Materials (SM).

In the early stage of the LDIR analysis, we attempted to scan a large area of slide M032 in one run. The run was terminated by the software after a few hours when the scanned area reached 650 mm^2, about one-third of the entire area of the slide, with total particle counting to 17,305. Subsequently, we randomly selected 20 square fields, each being approximately 2.5 mm × 2.5 mm, for each slide in later analyses, with the total scanned area of about 130 mm^2 or 8% of the total slide area.

2.6. Calculations

The original particle counts on the slides by the LDIR were converted to the concentrations in particle counts per gram of sediment dry weight (p/g dw):

$$\text{Concentration} = (N - N_b) \times \left(\frac{1875}{A}\right)/m \quad (1)$$

where 1875 mm^2 (=25 mm × 75 mm) is the area of the entire slide, and m is the mass of the dry sample extracted in grams. Two methods were used with equation (1). In Method-1, N and N_b are the *original* counts in the sample and the procedural blank, respectively; and *A* is the *cumulative* area of the field counted in mm^2. In Method-2, N and N_b are the *average* counts of the 20 (22 for the matrix blank, or sand) fields randomly selected on slide of the sample and the procedural blank, respectively; and *A* is the *average* area of the fields in mm^2. The calculation was specific to each type (identity) of particle.

2.7. Quality control

No particles were found in the LDIR instrument blank. In order to evaluate potential sample contamination, four other types of blanks were analyzed. The "slide blank" was an original MirrIR slide that was placed on a bench in our laboratory and exposed to air for four days. A "methanol blank" was prepared by spreading drops of methanol on a slide that was then exposed to air for days. Both slide and methanol blanks were scanned for 10 field (about

Table 1
Concentrations of particles identified by LDIR (count per gram dry weight).[a]

	Method-1			Method-2		
	Sand	M009	M032	Sand	M009	M032
Dry weight extracted, g	30.0	22.0	20.8	30.0	22.0	20.8
Number of LDIR fields	22	20	20	22	20	20
Cumulative field area, mm^2	129	134	155	129	134	155
	Microplastics					
Acrylates Polyurethanes Varnish	0.0	3.2	0.0	0.0	2.6	0.0
Acrylonitrile Butadiene	0.0	19.7	0.0	0.0	19.6	0.0
Ethylene Vinyl Acetate (EVA)	0.0	0.6	0.0	0.0	0.6	0.0
Polyacetal	44.6	29.2	17.4	39.5	29.0	16.6
Polyamide (PA)	65.9	268	186	56.1	266	180
Polybutadiene	0.0	0.0	0.6	0.0	0.0	0.60
Polycaprolactone	0.0	0.0	0.0	0.0	0.0	0.0
Polyester	34.4	132	93.6	27.4	130	86.0
Polyether	0.0	0.0	0.0	0.0	0.0	0.0
Polyethylene	0.0	0.0	0.0	0.0	0.0	0.0
Polyethylene Chlorinated	0.0	0.6	0.0	0.0	0.3	0.0
Polyethylene Terepthalate	1.9	0.0	0.0	1.6	0.0	0.0
Polyisoprene Chlorinated	0.0	1.3	0.0	0.0	1.3	0.0
Polylactic acid (PLA)	11.6	1.9	0.6	10.3	1.8	0.3
Polymethylmethacrylate (PMMA)	1.0	5.7	0.6	0.9	5.7	0.6
Polypropylene	0.0	2.5	0.0	0.0	2.2	0.0
Polystyrene	0.0	3.2	0.0	0.0	3.1	0.0
Polysulfones	1.0	0.0	0.0	0.9	0.0	0.0
Polytetrafluoroethylene (PTFE)	15.5	45.7	145	7.4	42.2	130
Polyvinyl alcohol	0.0	5.1	0.0	0.0	5.0	0.0
Polyvinyl Chloride (PVC)	1.5	5.1	0.0	1.3	5.1	0.0
Sum of microplastics	**178**	**524**	**444**	**146**	**515**	**414**
	Non-plastics and Unknowns					
Cellulose Chemically Modified	0.0	3.2	0.0	0.0	3.0	0.0
Chitin	0.0	55.8	7.0	0.0	55.8	6.9
Natural Polyamide	0.0	0.0	714	0.0	0.0	638
Rubber gaskets	0.0	87.6	0.0	0.0	86.9	0.0
Silica	3.4	3.8	0.0	3.0	3.8	0.0
Silicone	0.0	0.0	0.0	0.0	0.0	0.0
Unknown	0.0	436	378	0.0	417	301
	All Particles					
Total	**181**	**1110**	**1540**	**149**	**1080**	**1360**

[a] After subtraction of the counts in procedural blank, which had 20 counted fields with cumulative field area of 134 mm^2.

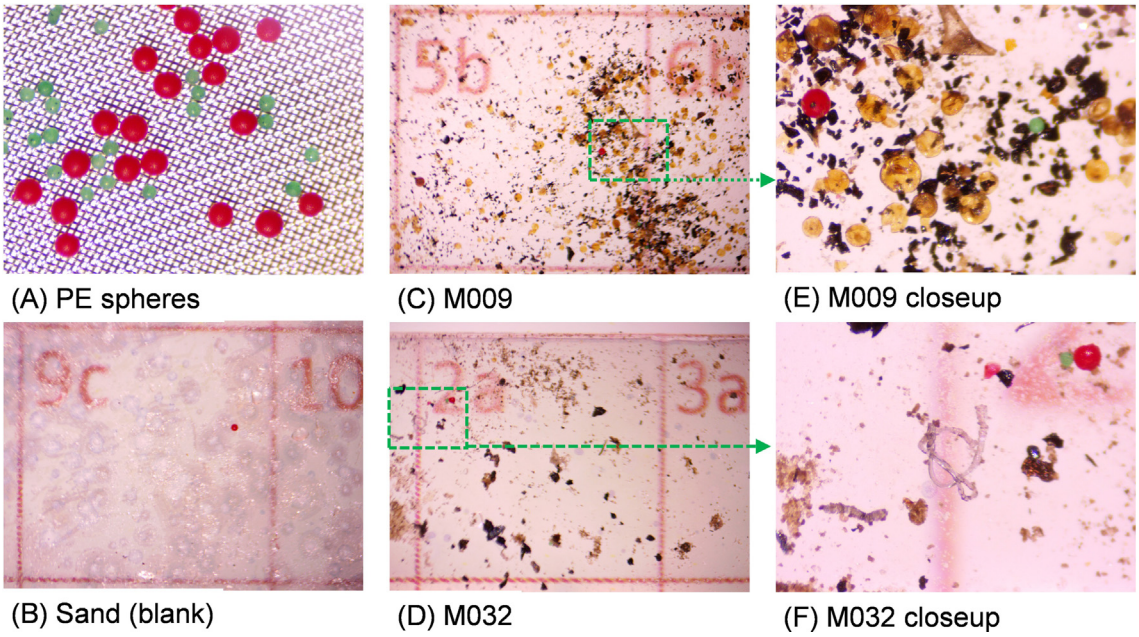

Fig 3. Example photos taken by the AmScope microscope. (A): Cospheric PE red and green spheres on 25 μm 316L stainless steel screen; (B): Sand (matrix blank); (C) and (D): One of 40 grids of the sediment samples M009 and M032, respectively, on a low P-E glass slide; (E) and (F): Close-up of C and D. In all these photos, the red sphere diameters were 212–250 μm, and the green sphere diameters were 106–125 μm. The squared cells shown in panels B, C, and D measured 7.5 mm × 7.5 mm. (For interpretation of the references to color in this figure legend, the reader is referred to the web version of this article.)

total 65 mm^2) by the LDIR, and found to have a negligible number of particles (totaling 21 and 18 particles, respectively) when compared with the numbers found in sediment samples. A "procedural blank" was run through all the steps in the procedure with no solid sample matrix. A commercial sand sample (CAS#14808–60-7, Silica Sand Natural Grain, US Silica) was processed along with sediment samples as a "matrix blank". The particle counts for individual chemical identity groups in the procedural blank were used to correct the corresponding counts in samples.

The red and green Cospheric microspheres were added to each sample and the procedural and matrix blanks, before starting the initial density separation. Fig. 3 shows the Cospheric PE spheres on the 25-μm stainless steel net. The red spheres on each prepared MirrIR slide were counted under the AmScope microscope, and the numbers in all grid cells of each slide were summed to calculate the analytical recovery. The recoveries of the red spheres in all samples (N = 9, including 8 samples + 1 duplicate of M009) were in the range of 50%–107%, with an average (±standard deviation) of 71(±20)%. The surrogate recoveries were used to evaluate potential sample losses, but were not used to adjust the results reported below. The green PE microspheres were found useful in providing a reference of the sizes during the stereomicroscope examination; however, their handling and counting were difficult even under the microscope due to the small particle size. Sediment M009 was processed in duplicates. The relative standard deviation of the surrogate recoveries for the duplicates were 4%.

3. Results and discussion

Selected photos taken by the AmScope stereomicroscope are presented in Fig. 3, and additional photos are presented in Fig. S1 of the SM. Numerous particles of different sizes and shapes were found (Fig. 3-C to 3-F). The matrix blank (sand) appeared to have relatively few particles except the added red PE spheres (Fig. 3B). The stereomicroscope allowed visualization of the color, the size, and, to some extent, the three-dimensional shape of the particles. However, the large number of particles made the use of stereomicroscope impractical to count particles in the sediment samples of this work.

LDIR data have been acquired for all four blanks and only two sediment samples M009 and M032 because of the laboratory facility was closed after the outbreak of COVID-19 pandemic. Photos of these six slides, as appeared on the LDIR software screen, are displayed in Fig. S2 of the SM. After a scan area was selected, the data acquisition was highly automated at about 7.2 sec per particle (Fig. S3 in the SM). Scanning of the slides of the two sediment samples took about 6 h and 8 h, respectively, with average scan time of about 20 min for each of the 20 square fields. During the run, information of the polymer identities as well as the size and shape were displayed along with the IR spectrum for each particle (Fig. 4). At the end of each run, a number of data files, including image data of each scanned field (CSV, PNG, Envi or PDF files), particle data (CSV or Microsoft Excel files), and spectra data (CSV files), were provided.

3.1. Counts and sizes of the microplastic particles

After subtracting the number of MP particles in the procedural blank, about 520p/g dw and 430p/g dw were found in the samples M009 and M032, respectively; and the results from using two different calculation methods agreed well (Table 1). Sampling site M032 was located in the northern basin of the lake, where the water depth was 257 m, the sediment mass accumulation rate (MAR) was 0.018 ± 0.002 g/cm^2-y, and the focusing factor (FF) was 1.2 (Corcoran et al., 2018). Water gyres and bottom currents are known to transport plastic debris, fibers, and fragments from shore to deep spots in the oceans (Kane et al., 2020; Peng et al., 2020) and other large lakes (Xiong et al., 2018). Sampling site M009 was at the southeast side of Lake Michigan, about 16 km from shore with a water depth of 62 m. The site is in a depositional zone with MAR of 0.065 ± 0.005 g/cm^2-y and FF > 2 (Corcoran et al., 2018), and is a pollution "hotspot" with high concentrations of many legacy and emerging pollutants (Cao et al., 2017; Christensen et al., 2019; Codling et al., 2018; Codling et al., 2014; Guo et al., 2016; Guo et al., 2017; Guo et al., 2020; Guo et al., 2014; Li et al., 2018; Peng et al., 2016a; Peng et al., 2016b). Although the assessment of MP pollution in Lake Michigan is beyond the scope of this work, our results clearly indicated that the lake is contaminated with microplastics. This is in accordance with the findings of previous MP studies for the water and sediment in the tributaries and other locations of the lake (Baldwin et al., 2016; Lenaker et al., 2019; Lenaker et al., 2021; Mason et al., 2016; McCormick et al., 2014; Peller et al., 2019).

The analysis MPs becomes more difficult for smaller sizes, especially in complex matrices such as natural sediment. In this work, we counted and characterized the particle as small as 20 μm (Table S1b in the SM), which is smaller than those found in many other studies on MPs in freshwater sediments (Yang et al., 2021). The "diameter" data provided by LDIR is the circular equivalent diameter, which is the square root of ($4/\pi \times$ measured area). Among all the MP particles detected by LDIR (N = 5769), the median diameter was 50 μm (Table S1a in the SM), and 84% and 96% of them had diameters below 100 μm and 250 μm, respectively. Fig. S4 in the SM illustrates the histograms for all detected particles and the sum of MPs. Information about size range, especially the lower limit, is often not available in published studies. In others, individual MPs with size as small as a few microns were presented but the counts and/or concentrations are not given. In addition, studies using saturated NaCl solution for density separation could have missed MPs heavier than 1.2 g/cm^3. The inconsistency in laboratory methods, targeted particle size ranges, instrument sensitivity, and reporting unit makes it impossible to compare the levels of contamination reported from different studies (He et al., 2020; Van Cauwenberghe et al., 2015).

Smaller MPs occurred in much greater numbers in the sediments of this work, similar to the finding in the water of the Great Lakes (Cable et al., 2017). Particle counts increased with decreasing particle sizes and followed a power law curve (Kooi and Koelmans, 2019), as shown by the log–log plot in Fig. 5 for the data of this work. The exponent value for the sum of MPs was 1.7, which is similar to the average 1.6 based on 19 data sets obtained from various waters and sediments (Kooi and Koelmans, 2019). This suggests that, if the diameter is halved, the count (or concentration) would increase by a factor of about 3.3, suggesting that a large portion of the smaller MPs was generated by the breakdown of larger plastic pieces. The fragmentation and degradation of polymer particles down to nanoparticles, as well as the mechanisms of these processes, have been discussed by Mattsson et al. (2015). The evidence of oxidative and mechanical weathering of plastics particles have also been previously provided (Zhang et al., 2016).

3.2. Identities and morphologies of the microplastic particles

Tables S1a and S1b in the SM present the descriptive statistics of the size and shape parameters of all particles by identity (N = 25,384). Most of the particles were those in the large scan area of slide M032L (N = 17,305). A total of 21 identities of MP particles were found by the LDIR system. Examples of the spectra for the four major MP identifications are given in Fig. S5 of the SM. Overall, polyamide was the most abundant microplastic, followed by polyester, polytetrafluoroethylene (PTFE), and polyacetal (Table 1).

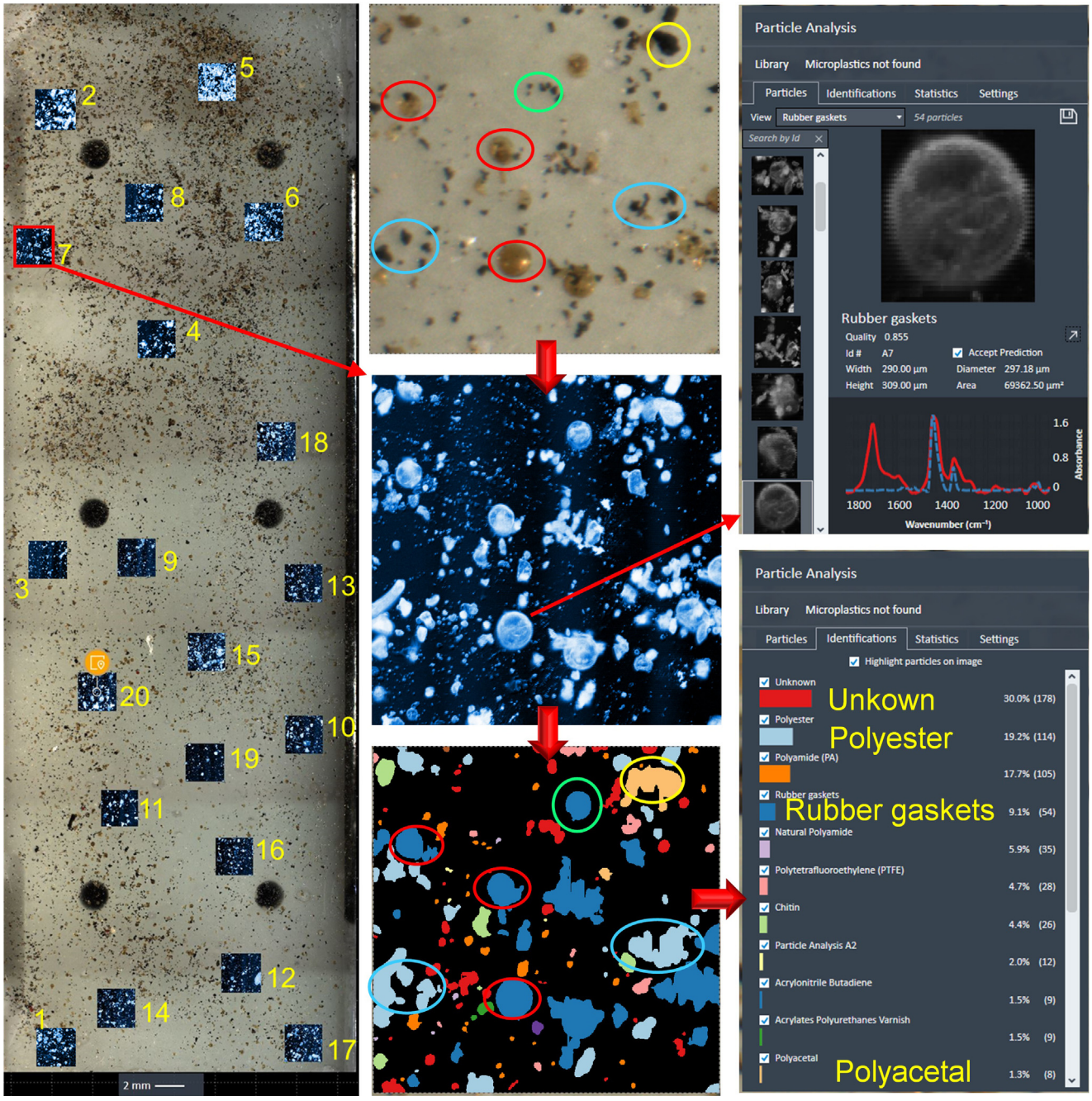

Fig. 4. The MirrIR low-e glass slides for samples M009, with 20 randomly selected fields marked for LDIR analyses (left panel). The entire area of each slide is 25 mm × 75 mm. The 20 selected grids are approximately 2.5 mm × 2.5 mm each. The images in the middle are close-ups of field No. 7 (as an example), including the original photo taking with visible light (top), the original image scanned by LDIR (middle), and the color highlighted image discerning polymer identities (bottom). Each particle was identified by comparation with the spectra in the spectral library (upper right panel). The relative abundances of different particles found in a field were presented (bottom right panel).

All these major MPs have densities greater than one. We noticed that polyethylene and polypropylene, both having densities of <1, were found to be the dominant plastic particles in the pelagic water of Lake Michigan (Mason et al., 2016). The difference in dominant plastic types between water and sediment could be attributed to the difference in buoyancy, which is related to density (Cable et al., 2017; Lenaker et al., 2019). In addition, it is known that some polymers, including low density polyethylene, could react with 30% hydrogen peroxide (Anderson et al., 2017), which has been widely used in environmental MP studies and was used in this work.

The differences in morphological parameters among the four major MPs were analyzed by Mann-Whitney U Test (Wilcoxon Rank Sum Test), which revealed that polyamide is significantly different from polyacetal and polyester in all the dimensional and morphological parameters, but largely similar with PTFE (Table S2 in the SM). In general, polyamide particles are larger than other MP types (Table S2 in the SM). In most MP research, the particles are categorized into fragments, fiber, bead, film, etc., but rigorous classifications based on measured morphologic parameters are not often provided. Given that spectroscopic measurements rely on light projection and absorption, caution is needed to

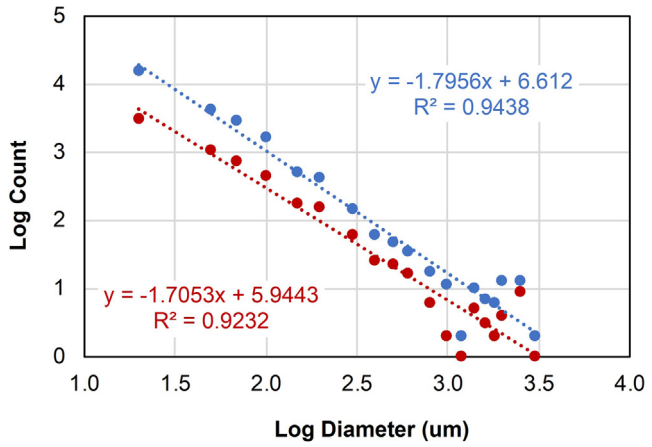

Fig. 5. Relative microplastic abundance for different particle size ranges. Blue dots and regression are for all particles, and red ones are for all MPs detected in this work. The diameter in the x-axis label is the lower cut-off diameter ranges, i.e., the size bin values of the histograms shown in Fig. S4 of the Supplementary Materials. (For interpretation of the references to color in this figure legend, the reader is referred to the web version of this article.)

compare the dimensional and morphological parameters provided by the LDIR software with those used in the literature (Kooi and Koelmans, 2019). Here, we roughly defined "fiber" for particles with an aspect ratio ≥3 (ATSDR, 2004), "bead" for particles with circularity >0.9 (Scircle et al., 2020), and "fragment" for all other particles. In assigning "fiber", we allowed the aspect ratio to be either "width / height" (as reported by LDIR) or "height / width". This categorization resulted in 153 (2.7%) fiber, 180 (3.1%) beads, and 5436 (94%) fragments, among total 5769 MP particles detected in all samples. In the waters of rivers, including the tributaries of the Great Lakes, fiber was found to be the dominant form of MPs (Baldwin et al., 2016; McCormick et al., 2016). Fibers have also been found to be abundant on ocean floors (Kane et al., 2020; Thompson et al., 2004). The transport and fates of MPs in natural waters, including buoyance and settling behaviors, may be largely influenced by the particle shape in addition to size and density (Waldschlager and Schuttrumpf, 2019). Although difficult to confirm in this study, loss of fibers during sample treatment could occur, as fibers may be more likely to attach to the glassware and sink during density separation, and could also pass the openings of the stainless steel screen during the multiple filtration steps.

3.3. Non-plastic and unidentified particles

About 14% and 46% of all particles in M009 and M032, respectively, were non-plastic and identified as natural polyamide, chemically modified cellulose, chitin, silica, silicate, or rubber gasket materials. The spectra of natural polyamide and rubber gasket are included in Fig. S5 of the SM. Among identified particles, natural polyamide had the highest count in sample M032. Naturally occurring polyamide includes proteins which are rich in sediment organic matter as an important nutrient source for benthic deposit feeders. Many particles that appeared as gold-colored spheres under the stereomicroscope in sample M009 (Fig. 4) were identified by the LDIR as "rubber gasket" (Fig. S6-A in the SM). The source of these rubber particles is unknown.

In sediment samples, 39% in M009 and 25% in M032 of the blank-subtracted total numbers of particles were not identified by the LDIR thus reported as "unknown". The lack of identification for many particles by the software is likely due to coagulation or aggregation of multiple particles on the MirrIR slides, producing mixed spectra. In a number of cases, the added surrogate red and green Cospheric PE spheres were reported as unknowns, because they were overlaid with other particles. Additionally, if the particle had sustained significant degradation, so that new spectral bands were present or morphological changes occur distorting peak shapes, an unknown classification might be returned.

Visual inspection of the MirrIR slides (Fig. 3, Fig. S1 and Fig. S2 in the SM) found large numbers of black colored particles in M009 and, to a lesser extent, M032. They were largely absent in the slides of the matrix blank (sand) and other blanks. Most of these black colored particles were irregular and similar to or smaller than the reference green Cospheric PE spheres of diameter 106–125 μm. As shown in Fig. S6-B of the SM, most of these black particles were identified as "unknown", although a few as polyester or polyacetal. Black carbon (BC) produced from incomplete combustions of fuels and other organic matter have been found in the sediments of Lake Michigan (Bonina et al., 2018; Goldberg et al., 1981; Griffin and Goldberg, 1981). With a density ranging 1.2–1.8 g/cm^3 (Long et al., 2013), BC particles may not be completely separated from microplastics during the $ZnCl_2$ density separation steps. The H_2O_2 oxidation and acid digestion might transform but cannot destroy BC particles. Therefore, it is possible that a good portion of the BC particles in the sediment survived the laboratory process and deposited on the MirrIR slides. BC particles could not be identified because the spectrum for BC is not available in the LDIR spectra library.

3.4. Potential bias and uncertainties

Few particles were found in the slide blank and methanol blank, and most of them were "unknown". This may suggest that deposition of particles from the laboratory air onto the slides was minimal. However, although the MirrIR slide for our procedural blank looks relatively "clean" visually (Fig. S2 in the SM), >1000 particles were found by the LDIR, including natural polyamide (37.3%), "unknown" (36.5%), PTFE (7.3%), polyethylene (4.6%), and polyamide (3.2%). Similar counts and identities resulted from the analysis of the matrix blank "sand". These suggest the presence of contamination sources in our laboratory, even though most of the particles found in the procedural and matrix blanks were not plastic.

It was impractical to count and characterize all particles on the entire MirrIR slides for this work. Given the uneven distribution of the particles on the slides, sufficient area should be scanned to ensure the final count is within the desired accuracy for the whole sample. In this work, we found that the relative standard deviation (RSD) for the cumulative total particle count decreased to <20% when the number of scanned fields was increased to 20 (about 8% of the total area of a slide) for all samples including the procedural and matrix blanks and sediments M009 and M032.

Agglomeration and aggregation of particles could affect counting and result in failed or erroneous identifications. The presence of a significant amount of carbon particles may also attenuate the IR light, thus affect the generation and lower the quality of spectra for MPs. Agglomeration and aggregation may be lessened by taking additional steps in sample preparation, such as sonication (Scircle et al., 2020). Taking additional steps to eliminate non-plastic particles, which could not be separated based on their densities, is desired.

Using surrogate addition for recoveries and method evaluation is helpful. However, using PE may biases the finding, as they have a density of about 0.98. Moreover, other polymers (polyester, polyamides, PVC, etc) have varied densities and are not represented by PE in the density separation. Spheres are also more buoyant than other particles of same volume but different surface areas, which can impact separation efficiency. In contrast, spheres are also more readily lost from a flat surface like a slide as they roll easily. There-

fore, using a series of surrogates with varied density and shapes would improve analytical accuracy in the future study.

4. Conclusions

Presented in this paper are our first-hand experience using the laser direct infrared (LDIR) spectrometry on the characterization and quantification of microplastic particles in natural sediment. Compared with FTIR which has been used widely in research on environmental plastics, LDIR is significantly faster thus allows the characterization of larger number of particles in high-throughput MP analysis. In this work, we counted and characterized all the detected MP particles, with diameters as small as 20 μm which has not been often reported for natural sediment samples. We showed that the number of MP particles increased rapidly with decreasing particles size, and quantified such increase with a power law equation. Additionally, we showed that the removal of non-plastic particles during sediment extraction and digestion may not be complete; their exclusion in the quantification of MPs in complex sample matrices would rely on the identification by LDIR or other instrument of similar capability. Based on these observations, we expect to see growing uses of LDIR in environmental particle research and the standardization of environmental MP analysis based on advanced technologies in the future.

CRediT authorship contribution statement

Yi-Ling Cheng: Methodology, Data curation, Writing – original draft. **Ruijie Zhang:** Methodology, Writing – original draft, Writing – review & editing. **Louis Tisinger:** Methodology, Writing – review & editing. **Salvatore Cali:** Methodology, Writing – review & editing. **Zhou Yu:** . **Hua Yun Chen:** Data curation. **An Li:** Conceptualization, Methodology, Writing – review & editing, Funding acquisition, Project administration, Supervision.

Declaration of Competing Interest

The authors declare that they have no known competing financial interests or personal relationships that could have appeared to influence the work reported in this paper.

Acknowledgment

This work was funded by a seed fund from the Illinois/Indiana Sea Grant (IISG) College Program of the U.S. National Oceanic and Atmospheric Administration (NOAA) [grant number NA18OAR4170082]. Funding was also received from the Dean's Office of the School of Public Health and the Division of Environmental and Occupational Health Sciences at the University of Illinois at Chicago. Dr. Li is partially supported by the Samuel and Catherine Epstein Professorship. Mr. Cali's participation was supported by the National Institute for Occupational Safety and Health Grant #T42/OH008672. Dr. Chen's participation was supported by National Institutes of Health/National Institute of Environmental Health Sciences, Grant P30ES027792 Chicago Center for Health and Environment (CACHET). Sediment sampling was part of the Great Lakes Sediment Surveillance Program funded by U.S. EPA Great Lakes Restoration Initiative (Assistance No. GL-00E00538). The contents of this paper are solely the responsibility of the authors and do not necessarily represent the official views of the funders. We thank Dr. Gary J. Laughlin and Mr. Sebastian B. Sparenga at McCrone Research Institute in Chicago, as well as the scientists at Illinois Public Health Laboratories for their assistance and helpful discussions.

Appendix A. Supplementary material

Supplementary data to this article can be found online at https://doi.org/10.1016/j.gr.2021.10.002.

References

Alimi, O.S., Farner Budarz, J., Hernandez, L.M., Tufenkji, N., 2018. Microplastics and nanoplastics in aquatic environments: aggregation, deposition, and enhanced contaminant transport. Environ. Sci. Technol. 52 (4), 1704–1724.

Anderson, P.J., Warrack, S., Langen, V., Challis, J.K., Hanson, M.L., Rennie, M.D., 2017. Microplastic contamination in Lake Winnipeg, Canada. Environ. Pollut. 225, 223–231.

Andrady, A.L., 2011. Microplastics in the marine environment. Mar. Pollut. Bull. 62 (8), 1596–1605.

ATSDR, 2004. Toxicological Profile For Synthetic Vitreous Fibers. Agency for Toxic Substances and Disease Registry. September 2004. https://www.atsdr.cdc.gov/ToxProfiles/tp.asp?id=908&tid=185 (accessed July 11, 2020).

Baldwin, A.K., Corsi, S.R., Mason, S.A., 2016. Plastic debris in 29 great lakes tributaries: relations to watershed attributes and hydrology. Environ. Sci. Technol. 50 (19), 10377–10385.

Bonina, S.M.C., Codling, G., Corcoran, M.B., Guo, J., Giesy, J.P., Li, A., Sturchio, N.C., Rockne, K.J., 2018. Temporal and spatial differences in deposition of organic matter and black carbon in Lake Michigan sediments over the period 1850–2010. J. Great Lakes Res. 44 (4), 705–715.

Browne, M.A., Crump, P., Niven, S.J., Teuten, E., Tonkin, A., Galloway, T., Thompson, R., 2011. Accumulation of microplastic on shorelines worldwide: sources and sinks. Environ. Sci. Technol. 45, 9175–9179.

Cable, R.N., Beletsky, D., Beletsky, R., Wigginton, K., Locke, B.W., Duhaime, M.B., 2017. Distribution and modeled transport of plastic pollution in the great lakes, the world's largest freshwater resource. Front. Environ. Sci. 5, 45.

Cao, D., Guo, J., Wang, Y., Li, Z., Liang, K., Corcoran, M.B., Hosseini, S., Bonina, S.M.C., Rockne, K.J., Sturchio, N.C., Giesy, J.P., Liu, J., Li, A., Jiang, G., 2017. Organophosphate esters in sediment of the great lakes. Environ. Sci. Technol. 51 (3), 1441–1449.

Christensen, E.R., Zhang, R., Codling, G., Giesy, J.P., Li, A., 2019. Poly- and perfluoroalkyl compounds in sediments of the Laurentian Great Lakes: loadings, temporal trends, and sources determined by positive matrix factorization. Environ. Pollut. 255, 113166. https://doi.org/10.1016/j.envpol.2019.113166.

Codling, G., Hosseini, S., Corcoran, M.B., Bonina, S., Lin, T., Li, A., Sturchio, N.C., Rockne, K.J., Ji, K., Peng, H., Giesy, J.P., 2018. Current and historical concentrations of poly and perfluorinated compounds in sediments of the northern Great Lakes – Superior, Huron, and Michigan. Environ. Pollut. 236, 373–381.

Codling, G., Vogt, A., Jones, P.D., Wang, T., Wang, P., Lu, Y.-L., Corcoran, M., Bonina, S., Li, A., Sturchio, N.C., Rockne, K.J., Ji, K., Khim, J.-S., Naile, J.E., Giesy, J.P., 2014. Historical trends of inorganic and organic fluorine in sediments of Lake Michigan. Chemosphere 114, 203–209.

Corcoran, M., Sherif, M.I., Smalley, C., Li, A., Rockne, K.J., Giesy, J.P., Sturchio, N.C., 2018. Accumulation rates, focusing factors, and chronologies from depth profiles of 210Pb and 137Cs in sediments of the Laurentian Great Lakes. J. Great Lakes Res. 44 (4), 693–704.

Driedger, A.G.J., Dürr, H.H., Mitchell, K., Van Cappellen, P., 2015. Plastic debris in the Laurentian Great Lakes: a review. J. Great Lakes Res. 41 (1), 9–19.

Dris, R., Imhof, H.K., Löder, M.G.J., Gasperi, J., Laforsch, C., Tassin, B., 2018. Chapter 3 - Microplastic Contamination in Freshwater Systems: Methodological Challenges, Occurrence and Sources. In: Zeng, E.Y. (Ed.), Microplastic Contamination in Aquatic Environments. Elsevier, pp. 51–93.

Goldberg, E.D., Hodge, V.F., Griffin, J.J., Koide, M., Edgington, D.N., 1981. Impact of fossil-fuel combustion on the sediments of lake-Michigan. Environ. Sci. Technol. 15 (4), 466–471.

Griffin, J.J., Goldberg, E.D., 1981. Sphericity as a characteristic of solids from fossil-fuel burning in a lake-Michigan sediment. Geochim. Cosmochim. Ac. 45 (5), 763–769.

Guo, J., Li, Z., Ranasinghe, P., Bonina, S., Hosseini, S., Corcoran, M.B., Smalley, C., Kaliappan, R., Wu, Y., Chen, D.a., Sandy, A.L., Wang, Y., Rockne, K.J., Sturchio, N.C., Giesy, J.P., Li, A., 2016. Occurrence of atrazine and related compounds in sediments of upper great lakes. Environ. Sci. Technol. 50 (14), 7335–7343.

Guo, J., Li, Z., Ranasinghe, P., Bonina, S., Hosseini, S., Corcoran, M.B., Smalley, C., Rockne, K.J., Sturchio, N.C., Giesy, J.P., Li, A., 2017. Spatial and temporal trends of polyhalogenated carbazoles in sediments of upper great lakes: insights into their origin. Environ. Sci. Technol. 51 (1), 89–97.

Guo, J., Li, Z., Ranasinghe, P., Rockne, K.J., Sturchio, N.C., Giesy, J.P., Li, A., 2020. Halogenated flame retardants in sediments from the Upper Laurentian Great Lakes: implications to long-range transport and evidence of long-term transformation. J. Hazard. Mater 384, 12.

Guo, J., Chen, D., Potter, D., Rockne, K.J., Sturchio, N.C., Giesy, J.P., Li, A., 2014. Polyhalogenated carbazoles in sediments of Lake Michigan: a new discovery. Environ. Sci. Technol. 48 (21), 12807–12815.

He, B., Goonetilleke, A., Ayoko, G.A., Rintoul, L., 2020. Abundance, distribution patterns, and identification of microplastics in Brisbane River sediments, Australia. Sci. Total Environ. 700, 134467. https://doi.org/10.1016/j.scitotenv.2019.134467.

Isobe, A., Buenaventura, N.T., Chastain, S., Chavanich, S., Cózar, A., DeLorenzo, M., Hagmann, P., Hinata, H., Kozlovskii, N., Lusher, A.L., Martí, E., Michida, Y., Mu, J., Ohno, M., Potter, G., Ross, P.S., Sagawa, N., Shim, W.J., Song, Y.K., Takada, H., Tokai, T., Torii, T., Uchida, K., Vassillenko, K., Viyakarn, V., Zhang, W., 2019. An interlaboratory comparison exercise for the determination of microplastics in standard sample bottles. Mar. Pollut. Bull. 146, 831–837.

Kaiser, D., Kowalski, N., Waniek, J.J., 2017. Effects of biofouling on the sinking behavior of microplastics. Environ. Res. Lett.

Kane, I.A., Clare, M.A., Miramontes, E., Wogelius, R., Rothwell, J.J., Garreau, P., Pohl, F., 2020. Seafloor microplastic hotspots controlled by deep-sea circulation. Science 368 (6495), 1140–1145.

Kole, M.R., Mainali, D., 2019. Rapid, Automated Analysis of Microplastics Using Laser Direct Infrared Imaging and Spectroscopy. Agilent Technologies, Inc.

Kevley Technologies, 2017. Home of MirrIR low-e microscope slides. http://kevley.com/

Kooi, M., Koelmans, A.A., 2019. Simplifying microplastic via continuous probability distributions for size, shape, and density. Environ. Sci. Tech. Let. 6 (9), 551–557.

Kooi, M., Nes, E.H.V., Scheffer, M., Koelmans, A.A., 2017. Ups and downs in the ocean: effects of biofouling on vertical transport of microplastics. Environ. Sci. Technol. 51 (14), 7963–7971.

Law, K.L., Thompson, R.C., 2014. Microplastics in the seas. Science 345 (6193), 144–145.

Lenaker, P.L., Baldwin, A.K., Corsi, S.R., Mason, S.A., Reneau, P.C., Scott, J.W., 2019. Vertical distribution of microplastics in the water column and surficial sediment from the Milwaukee River Basin to Lake Michigan. Environ. Sci. Technol. 53 (21), 12227–12237.

Lenaker, P.L., Corsi, S.R., Mason, S.A., 2021. Spatial distribution of microplastics in surficial benthic sediment of Lake Michigan and Lake Erie. Environ. Sci. Technol.

Li, A., Guo, J., Li, Z., Lin, T., Zhou, S., He, H., Ranansinghe, P., Sturchio, N.C., Rockne, K. J., Giesy, J.P., 2018. Legacy polychlorinated organic pollutants in the sediment of the Great Lakes. J. Great Lakes Res. 44 (4), 682–692.

Li, Q., Zeng, A., Jiang, X., Gu, X., 2021. Are microplastics correlated to phthalates in facility agriculture soil? J. Hazard. Mater. 412, 125164. https://doi.org/10.1016/j.jhazmat.2021.125164.

Long, C.M., Nascarella, M.A., Valberg, P.A., 2013. Carbon black vs. black carbon and other airborne materials containing elemental carbon: physical and chemical distinctions. Environ. Pollut. 181, 271–286.

Mason, S.A., Kammin, L., Eriksen, M., Aleid, G., Wilson, S., Box, C., Williamson, N., Riley, A., 2016. Pelagic plastic pollution within the surface waters of Lake Michigan, USA. J. Great Lakes Res. 42 (4), 753–759.

Masura, J., Baker, J., Foster, G., Arthur, C., 2015. Laboratory Methods for the Analysis of Microplastics in the Marine Environment: Recommendations for Quantifying Synthetic Particles in Waters and Sediments; NOAA Technical Memorandum NOS-OR&R-48; National Oceanic and Atmospheric Administration, Silver Spring, MD.

Mattsson, K., Hansson, L.A., Cedervall, T., 2015. Nano-plastics in the aquatic environment. 17, 1712–1721.

McCormick, A., Hoellein, T.J., Mason, S.A., Schluep, J., Kelly, J.J., 2014. Microplastic is an Abundant and Distinct Microbial Habitat in an Urban River. Environ. Sci. Technol. 48 (20), 11863–11871.

McCormick, A.R., Hoellein, T.J., London, M.G., Hittie, J., Scott, J.W., Kelly, J.J., 2016. Microplastic in surface waters of urban rivers: concentration, sources, and associated bacterial assemblages. Ecosphere 7 (11). https://doi.org/10.1002/ecs2.2016.7.issue-1110.1002/ecs2.1556.

Morét-Ferguson, S., Law, K.L., Proskurowski, G., Murphy, E.K., Peacock, E.E., Reddy, C. M., 2010. The size, mass, and composition of plastic debris in the western North Atlantic Ocean. Mar. Pollut. Bull. 60 (10), 1873–1878.

Peller, J.R., Eberhardt, L., Clark, R., Nelson, C., Kostelnik, E., Iceman, C., 2019. Tracking the distribution of microfiber pollution in a southern Lake Michigan watershed through the analysis of water, sediment and air. Environ. Sci.-Proc. Imp. 21 (9), 1549–1559.

Peng, H., Chen, C., Cantin, J., Saunders, D.M.V., Sun, J., Tang, S., Codling, G., Hecker, M., Wiseman, S., Jones, P.D., Li, A., Rockne, K.J., Sturchio, N.C., Giesy, J.P., 2016a. Untargeted screening and distribution of organo-bromine compounds in sediments of Lake Michigan. Environ. Sci. Technol. 50 (1), 321–330.

Peng, H., Chen, C., Cantin, J., Saunders, D.M.V., Sun, J., Tang, S., Codling, G., Hecker, M., Wiseman, S., Jones, P.D., Li, A., Rockne, K.J., Sturchio, N.C., Cai, M., Giesy, J.P., 2016b. Untargeted screening and distribution of organo-iodine compounds in sediments from Lake Michigan and the Arctic Ocean. Environ. Sci. Technol. 50 (18), 10097–10105.

Peng, L., Fu, D., Qi, H., Lan, C.Q., Yu, H., Ge, C., 2020. Micro- and nano-plastics in marine environment: Source, distribution and threats - A review. Sci. Total Environ. 698, 134254. https://doi.org/10.1016/j.scitotenv.2019.134254.

Primpke, S., Wirth, M., Lorenz, C., Gerdts, G., 2018. Reference database design for the automated analysis of microplastic samples based on Fourier transform infrared (FTIR) spectroscopy. Anal. Bioanal. Chem. 410, 5131–5141.

Reisser, J., Shaw, J., Wilcox, C., Hardesty, B.D., Proietti, M., Thums, M., Pattiaratchi, C., Hays, G.C., 2013. Marine plastic pollution in waters around Australia: characteristics, concentrations, and pathways. PLoS ONE 8 (11), e80466. https://doi.org/10.1371/journal.pone.0080466.

Scircle, A., Cizdziel, J.V., Tisinger, L., Anumol, T., Robey, D., 2020. Occurrence of microplastic pollution at oyster reefs and other coastal sites in the Mississippi Sound, USA: impacts of freshwater inflows from flooding. Toxics 8 (2), 35. https://doi.org/10.3390/toxics8020035.

Thompson, R.C., Olsen, Y., Mitchell, R.P., Davis, A., Rowland, S.J., John, A.W.G., McGonigle, D., Russell, A.E., 2004. Lost at sea: Where is all the plastic? Science 304.

Van Cauwenberghe, L., Devriese, L., Galgani, F., Robbens, J., Janssen, C.R., 2015. Microplastics in sediments: a review of techniques, occurrence and effects. Mar. Environ. Res. 111, 5–17.

Waldschläger, K., Schüttrumpf, H., 2019. Effects of particle properties on the settling and rise velocities of microplastics in freshwater under laboratory conditions. Environ. Sci. Technol. 53 (4), 1958–1966.

Xiong, X., Zhang, K., Chen, X., Shi, H., Luo, Z., Wu, C., 2018. Sources and distribution of microplastics in China's largest inland lake – Qinghai Lake. 235, 899–906.

Yang, L., Zhang, Y., Kang, S., Wang, Z., Wu, C., 2021. Microplastics in freshwater sediment: a review on methods, occurrence, and sources. Sci. Total Environ. 754, 141948. https://doi.org/10.1016/j.scitotenv.2020.141948.

Zettler, E.R., Mincer, T.J., Amaral-Zettler, L.A., 2013. Life in the "Plastisphere": microbial communities on plastic marine debris. Environ. Sci. Technol. 47 (13), 7137–7146.

Zhang, K., Su, J., Xiong, X., Wu, X., Wu, C., Liu, J., 2016. Microplastic pollution of lakeshore sediments from remote lakes in Tibet plateau, China. Environ. Pollut. 219, 450–455.

Zobkov, M., Esiukova, E., 2017a. Microplastics in Baltic bottom sediments: quantification procedures and first results. Mar. Pollut. Bull. 114 (2), 724–732.

Zobkov, M.B., Esiukova, E.E., 2017b. Evaluation of the Munich Plastic Sediment Separator efficiency in extraction of microplastics from natural marine bottom sediments. Limnol. Oceanogr.: Meth 15 (11), 967–978.